Nuclear Instruments and Methods in Physics Research A 807 (2016) 47–55

Contents lists available at ScienceDirect

Nuclear Instruments and Methods in Physics Research A

journal homepage: www.elsevier.com/locate/nima

Tracking performance of GasPixel detectors in test beam studies

A.S. Boldyrev [a], F. Hartjes [b], N.P. Hessey [b], M. Fransen [b], S.P. Konovalov [c], W. Koppert [b], A. Romaniouk [d], E. Shulga [d], S.Yu. Smirnov [d], Y. Smirnov [d], E.Yu. Soldatov [d], V.O. Tikhomirov [c,d,*], H. Van der Graaf [b], K. Vorobev [d]

[a] Skobeltsyn Institute of Nuclear Physics, Lomonosov Moscow State University, Moscow, Russia
[b] NIKHEF, Amsterdam, Netherlands
[c] P.N. Lebedev Physical Institute, Russian Academy of Sciences, Leninsky prospect, 53, 119991 Moscow, Russia
[d] National Research Nuclear University "MEPhI", Moscow, Russia

ARTICLE INFO

Article history:
Received 7 June 2015
Received in revised form
12 October 2015
Accepted 26 October 2015
Available online 6 November 2015

Keywords:
Micro-pattern detectors
GasPixel detectors
Precise tracking

ABSTRACT

A combination of a pixel chip and a gas chamber (GasPixel detectors) opens new opportunities for particle detectors. GasPixel detectors consist of an electron drift volume, an amplification gap and an anode plane based on a semiconductor chip. This technology promises large benefits in high-energy charged-particle tracking. It allows reconstruction of a 3D image of a particle track segment in a single detector layer with high accuracy. Several prototypes of GasPixel detectors based on micromegas technology with different gas mixtures and drift gaps were studied in a test beam. A spatial resolution of 8 μm and angular accuracy of about 0.2° in a chip plane were obtained. A dedicated Monte Carlo simulation of GasPixel detectors shows good agreement with experimental data.

1. Introduction

Operating conditions and challenging demands of present and future accelerator experiments result in new requirements on detector systems, particularly to tracking detectors in the innermost part of experimental setups. High track density and particle rate in an inner tracking volume require radiation hard detectors with high granularity which would ensure not only an accurate momentum measurement but also robust pattern recognition and long-term operation without access. Modern experiments often operate at high trigger rate and one of the new requirements of inner detectors at the LHC is to supply a first level trigger for high transverse momentum tracks. Inner trackers in collider experiments often consist of many layers of silicon detectors giving precise measurement of particle tracks. These detectors have made great progress over recent years but there are still a lot of ongoing developments and searches for new technologies to further improve the properties of tracking detectors (see, e.g., [1–3] and references within).

One of the new promising technologies which can be an alternative to the semiconductor detectors is based on the recent developments of GasPixel detectors [4–9], see also a review [10]. These detectors can combine the best properties of silicon and gaseous detectors, providing high precision 3D track segments in a single detector layer.

Operation principle of these detectors is similar to that of Time Projection Chambers (see, e.g., [11] and references within) with a two-dimensional readout plane. Schematic view of the GasPixel detector is shown in Fig. 1. A specially treated pixel electronics chip is placed in the gas volume. The gas volume has a drift gap (width of the gap depends on exact detector requirements) and an electron multiplication region. Detectors might be based on a GEM [4] technology or on a micromegas technology as shown in Fig. 1 [5–9,12]. The micromegas based detectors have a planar region with high electric filed approximately of 50 μm wide, separated from the drift volume by a mesh or a grid. Primary ionization electrons, produced by a charged particle, drift towards the pixel chip, focused into the grid holes (Fig. 1) and are measured by the pixels of the chip. The position of the hit pixel gives two coordinates in the pixel plane, while the measured drift time gives a third coordinate of a primary ionization. Depending on the exact realization of the chip functionality it is possible to measure time or amplitude or both simultaneously if required. The charged particle track can be reconstructed from the measured ionization points, giving a precise measurement of a space point (the point where the particle crosses the pixel chip plane), the angle in the chip plane, and the angle of incidence to the chip plane (3D track segment).

Possibility to reconstruct 3D track segments has two important applications for tracking detectors. Usually tracking systems in collider experiments contain quite a few layers of the detectors,

* Corresponding author at: P.N. Lebedev Physical Institute, Russian Academy of Sciences, Leninsky prospect, 53, 119991 Moscow, Russia. Tel.: +7 499 132 6032; fax: +7 499 135 7880.
E-mail address: Vladimir.Tikhomirov@cern.ch (V.O. Tikhomirov).

http://dx.doi.org/10.1016/j.nima.2015.10.087
0168-9002/

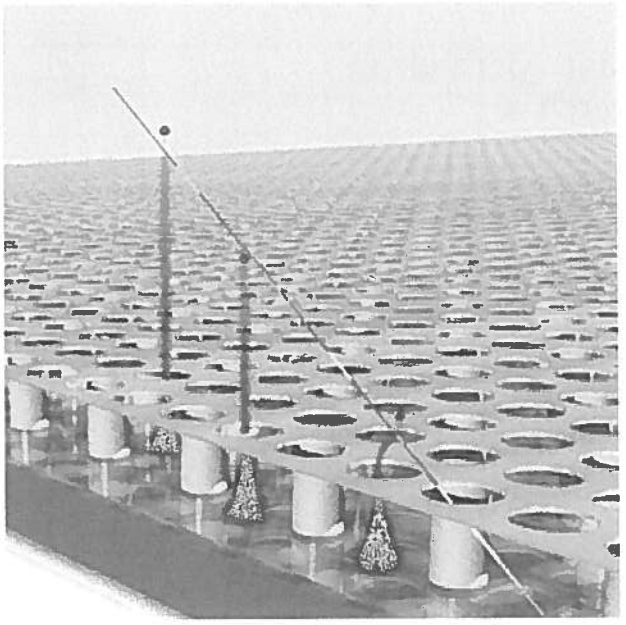

Fig. 1. Schematic view of the GasPixel detector. Primary ionization electrons produced by incident particle in gas volume drift down. The pixel chip in the bottom is separated from a drift volume by a mesh. Electron amplification happens in the gap between the mash and the pixel chip.

which measure space points (hits) on a particle track. At high particle track density many hit combinations are considered and finally all ambiguities are removed by iterative process of a track recognition. New technology allows us to provide not only a precise space point but using a tack segment in one detector layer it can predict a space point in the next layer of the tracking system, significantly reducing the number of combinations, and hence track reconstruction processing time ("vector" tracking). The second application is based on a specific feature of these detectors. When a particle traverses a gaseous volume it produces many ionization clusters. Diffusion makes drifting electrons to be collected by different pixels. In experiments operating at high trigger rate the amount of the information being sent to back-end electronics is too large and data must be compressed already at the front-end level. This means that basic data processing must be performed already on chip level, sending out only the track spatial coordinates and two angles. This processing can be carried out in a few tens of clock cycles, allowing the 3D segments to be used in a first level trigger system.

The GasPixel detectors design (gas composition, drift gap, and electronics) depends on the required functionality. For high energy physics application it can be a tracking only device or, filled with Xe-based gas mixture, may also combine tracking and transition radiation detector properties [8]. The detectors aimed to operate close to the interaction point and at high particle density should have a rather thin drift gap (1–2 mm) and use a fast and low diffusion gas mixture (see for instance [9]). If it is aimed to provide also a track segment (this paper) it should have a drift gap of 5–10 mm and a specially designed front-end electronics to be able to process data at the front-end level. It was shown that with low diffusion gas mixture a spatial resolution of GasPixel detectors is approaching 10 μm level [8,9]. Spatial resolution of about 8 μm is reached in this paper. For transition radiation (TR) registration the detector should have significant drift space (~20 mm) filled with Xe-based gas mixture for effective absorption of TR photons. The read-out electronics in this case should also measure the signal amplitude in each pixel. The advantage of GasPixel detectors as TRD devices is their capability to reconstruct a microscopic picture of ionization on the particle track and, hence, maximize separation between ionization and TR clusters.

GasPixel technique is at the beginning of its development but already now it finds applications in different areas, such as dual-phase noble gas Time Projection Chamber for dark matter search [13], low background single photon detector in the CAST experiment [14], X-ray polarimetry detector for X-ray astronomy [15], etc.

In this paper the results obtained in beam tests with several GasPixel prototypes dedicated for track measurements are presented. Section 2 describes the test beam set-up and the detector prototypes. In Section 3 a track reconstruction procedure and a method of a coordinate accuracy calculation are presented. Results of Monte Carlo (MC) simulations of a GasPixel detector are described in Section 4. Performance of the detector in the test beam experiments and comparison with MC are presented in Section 5. Conclusions are given in Section 6.

2. Test beam set-up

GasPixel test beam prototypes were built on the basis of Timepix-1 chips [16] with the pixel size of 55 × 55 μm^2. The chips have a 256 × 256 pixel matrix providing ~14 × 14 mm^2 sensitive area. The chips were protected against discharges by a 8 μm Si_3N_4 protection layer. The mesh was made using InGrid technology [5–7,9]. After amplification and shaping the signal from each pixel is sent to the discriminator. A noise level of individual channel of this chip is about 110 electrons; a minimum discriminator threshold of about 500 electrons is required for proper operation of the chip. In the beam tests threshold corresponding to 600 electrons was used. The output of the discriminator is directed towards the digital part which contains a 100 MHz oscillator that can be used to measure the amount of charge in terms of signal time-over-threshold or to measure the time moment when a signal on a pixel goes over threshold (drift-time). In the beam tests only the drift-time measurement mode was used. The frequency of oscillator defines time measurement bin of 10 ns. The shaper of the Timepix-1 chip amplifier has a rise time of 100 ns. The charge produced by primary ionization electrons varies widely due to statistical fluctuations in the avalanche process. A combination of slow rise time and large gas gain fluctuations leads to a large time-walk effect which together with time measurement bin of 10 ns have significant influence on the drift time measurement accuracy and, hence, on track reconstruction accuracy in the drift plane. Further generations of Timepix chip will significantly improve timing characteristics of the amplifier and read-out chains [17].

A view of an assembled GasPixel detector is shown in Fig. 2.

Three different GasPixel prototypes were exposed to 180 GeV muons and 100 GeV pions in the H4 beam line at the SPS at CERN. The first prototype with a drift gap of 10 mm was filled with low-diffusion gas mixture containing dimethylether (DME) and CO_2 (43/57%). The DME-based gas mixture has a high ionization cluster density (≈ 45 primary interactions per cm) and very low diffusion of drifting electrons. The combination of these two properties together with a high sensitivity to one primary electron provides necessary conditions to achieve an excellent coordinate accuracy. However DME is a highly flammable gas and in some applications this may contradict safety requirements. Much more conventional Ar-based mixtures are widely used in different gaseous detectors. They are cheap, nonflammable and do not require special equipment to operate. On the other hand, Ar-based mixtures have larger diffusion coefficients and less cluster density (≈ 25 primary interactions per cm) and hence one expects worse coordinate accuracy compared to DME-based mixtures. In order to understand a tracking performance with Ar-based mixture

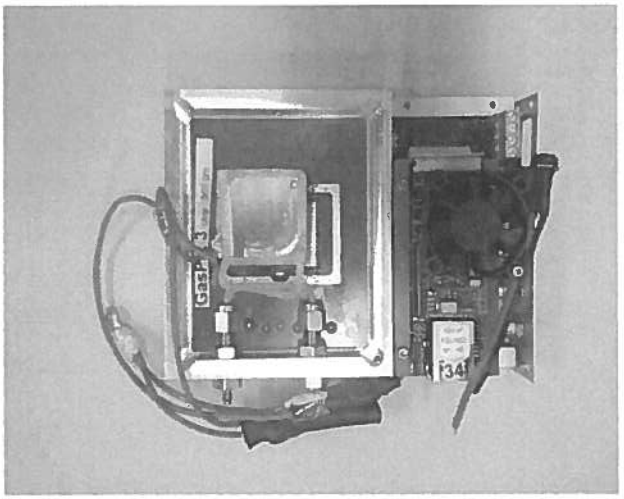

Fig. 2. Assembled GasPixel detector (left) connected to the front-end electronics (right).

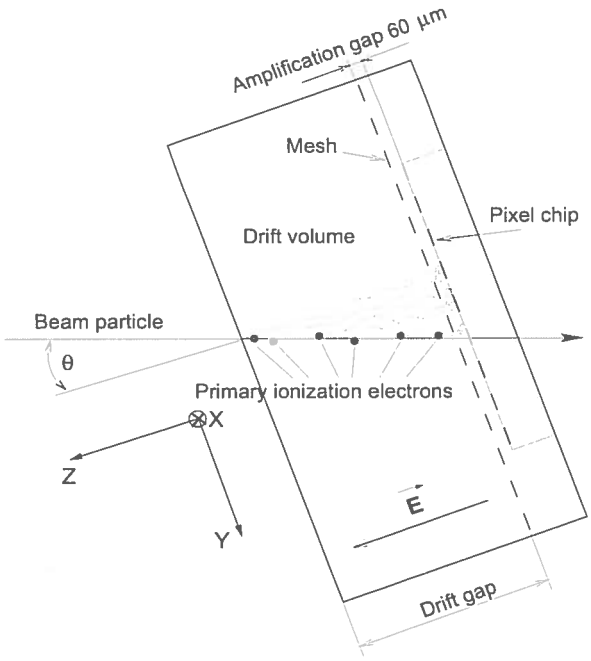

Fig. 3. Schematic view of the GasPixel detector exposed to the test beam.

dedicated studies with two detector prototypes with 5 mm and 10 mm drift gaps filled with Ar/CO_2-mixture (93/7%) were carried out.

GasPixel detector test beam geometry and operation principles are schematically shown in Fig. 3. The chambers were tilted with respect to the beam line in such a way that particles crossed it at angles θ of about 5°, 10°, 20° or 30° with respect to normal to the chip plane. Ionization electrons drift towards the pixel chip plane and create a track image on it. Coincidence of two scintillator counters with a size of about $13 \times 13\ mm^2$ (not shown in Fig. 3) provided a small beam spot on the tested detectors and was used as a trigger for the drift time measurements.

Fig. 4 shows a typical event display with DME-based gas mixture. The top figure shows a track projection on the pixel chip plane (X,Y coordinates). Each point corresponds to an individual fired pixel. The bottom figure is a result of reconstruction of a third coordinate in the

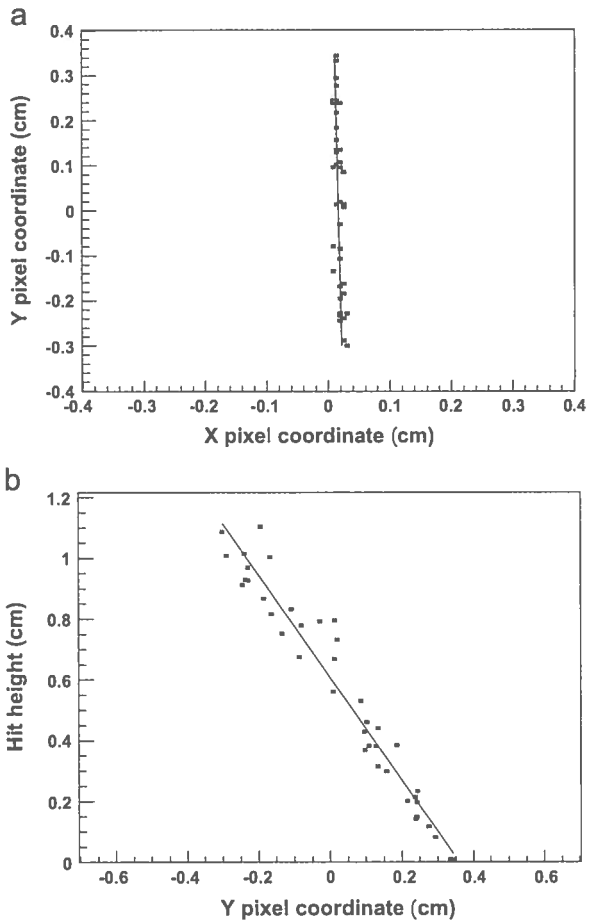

Fig. 4. Display of one event in the GasPixel detector filled with DME-based mixture: top – in the chip plane; bottom – in the plane orthogonal to the chip. Small boxes represent coordinates of hits: in the top view they correspond to the coordinates of fired pixels, for the bottom view the horizontal axis is pixel coordinate, the vertical axis is the third space point coordinate reconstructed using drift time measurements. Lines represent reconstructed tracks.

Table 1
Parameters of the prototypes and their working conditions used in the beam tests. E_{drift} – electric field in the drift region; U_{grid} – voltage of amplification gap between mesh and anode; V_{drift} – drift velocity; D_T and D_L – correspondingly transverse and longitudinal diffusion coefficients.

Parameter	Prototype 1	Prototype 2	Prototype 3
Drift gap (mm)	10	10	5
Pixel size (μm)	55	55	55
Gas mixture	DME/CO_2 43%/57%	Ar/CO_2 93%/7%	
E_{drift} (kV/cm)	3.5	1	
U_{grid} (V)	580	420	400
V_{drift} (cm/μs)	2.20	4.42	
D_T (μm/$\sqrt{cm}$)	72	430	
D_L (μm/$\sqrt{cm}$)	93	195	

plane perpendicular to the chip (Y,Z coordinates) using drift time measurements.

Parameters of GasPixel prototypes and their working conditions used in the beam tests are presented in Table 1. Drift velocities and diffusion coefficients were obtained with the Garfield program [18]. In all prototypes greed voltages were kept at the level which is safe for operation at the test beam conditions. These voltages allowed us to obtain the gas gain in the range of $1.5–2 \cdot 10^3$.

3. Tracking algorithms

In order to study tracking performance of the GasPixel prototypes, a dedicated track reconstruction procedure was developed. As a first step, the beam particle track is reconstructed as a straight line in two planes. In the chip plane (*X*,*Y* plane) the coordinates of centers of fired pixels are used for fitting. In the plane orthogonal to the pixel chip one coordinate corresponds to the pixel *Y* coordinate and another one is calculated from measured drift time using known drift velocity. Track fit parameters are obtained by the least squares method in several iterations. Some fraction of fired pixels (usually very small) were removed from the fitting procedure: "space outliers" (e.g. δ-electrons), "time outliers" (e.g., remnant of the second particle in the beam), and noisy pixels. Here the "space outliers" were defined as a hits with a distance to the reconstructed track above 3σ, where σ is an expected hit deviation due to diffusion. The "time outliers" were defined if the measured time of arrived signal exceeds maximum drift time (including possible longitudinal diffusion) for this GasPixel prototype. Pixels giving out a signal with frequency more than 10% of events were defined as noisy and excluded from analysis.

In order to take into account the diffusion effects each pixel coordinate is taken with its own weight in inverse proportion to the expected diffusion. Thus pixels closest to the track vertex (the point in which the particle crosses the chip plane) have low diffusion and hence larger contribution to coordinate measurement accuracy.

In the second step of the tracking procedure, beginning and end of the track projection are defined. Since the track projections on the chip plane were oriented mainly along *Y* axis, the projection boundaries were defined as *Y* coordinates of the first and the last fired pixels along the track projection. *X* coordinates of the track edges were then calculated from these *Y* boundaries using reconstructed track parameters.

Intrinsic coordinate resolution of the GasPixel detector is defined here as a difference between real coordinate of the point where beam particle crossed chip plane and reconstructed coordinate. Angular resolution is defined as a difference between real and reconstructed angles on the chip plane and on the plane normal to the chip. Since no beam tracking telescope with high enough precision was available as the reference for calculation of the track reconstruction accuracy, the so-called method of "odd–even tracks" was used [8,19]. The method is based on the artificial separation of tracking information in two independent interleaved parts: the first one consists of hits registered in odd rows of pixels, the second one – hits in even rows. Then in each event two particle tracks are reconstructed independently and their parameters are compared (Fig. 5).

Intrinsic resolution of the detector is by factor of 2 less than that obtained using difference of "odd" and "even" tracks (one $\sqrt{2}$ comes from the fact that a number of points on "odd" or "even" tracks is a factor of 2 less than on the "full" track and the other $\sqrt{2}$ – from subtraction procedure when the residual of parameters of these two tracks is defined). In Monte Carlo simulations, where true coordinates and angles are known, one can calculate the accuracy directly from parameters of the reconstructed track using all hits. Comparison of these direct results with those obtained by the "odd–even" technique confirms the general validity of the method. However there are some tiny effects which give slight biases in the "odd–even" method with respect to the direct one. For example, an uncertainty in a measurement of the intersection point along the *Y*-axis (4 in Fig. 5) leads to some additional error in the measurement of the *X* coordinate of this point. This error is the same for the "odd" and "even" tracks and it is largely canceled after the operation of subtraction. Fig. 6 compares the coordinate accuracy in *X* direction obtained by the direct and by the "odd–even" methods using MC simulations at different incident angles of the particle. One sees that for the test beam conditions at beam incident angles more than 10° the difference does not exceed

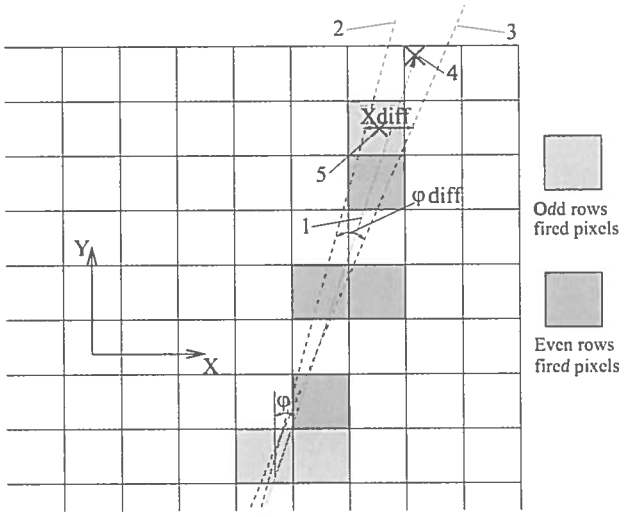

Fig. 5. Explanation of the "odd–even tracks" technique used to study tracking performance of the GasPixel detectors. 1 – Real track projection; 2 – reconstructed "odd track"; 3 – reconstructed "even track"; 4 – point of beam particle intersection with chip plane; 5 – center of the last fired pixel along track projection; ϕ – azimuth angle of a particle trajectory; Xdiff – difference of calculated *X* coordinates of reconstructed "odd" and "even" tracks; ϕdiff – difference of azimuth angles of reconstructed "odd" and "even" tracks.

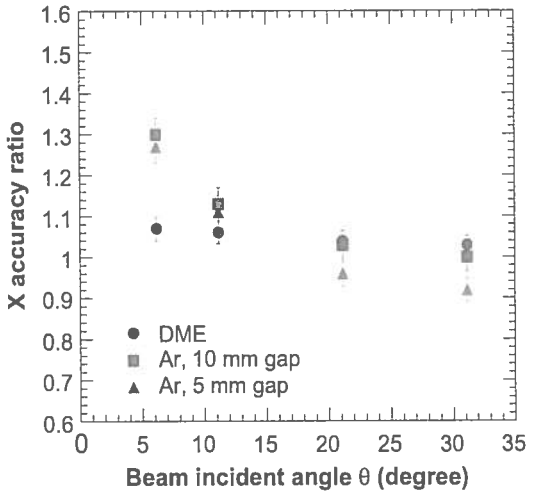

Fig. 6. Ratio of *X* coordinate accuracy obtained in MC by direct method (full track projection reconstruction) and calculated by "odd–even" technique. Results are presented for different prototypes and different incident angles of the beam.

10%. This fact allows us to conclude that the experimental accuracy obtained by the "odd–even" method is by 5–10% better than the real one. This should be considered as a systematic shift of the results presented in this paper.

The typical residual distributions of *X* coordinate and ϕ angle obtained by the "odd–even" method are shown in Fig. 7. The values presented in these histograms correspond to the expected accuracy, i.e. "odd–even" values are divided by a factor of 2, as explained above. The accuracy is defined as a σ of a Gaussian fit of the distribution core (range of $\pm 2\sigma$ around the peak position).

4. Monte Carlo simulations

In order to understand the test beam results the detailed Monte Carlo studies of each detector were performed for all experimental conditions. The MC simulations are based on the GEANT3 [20] and

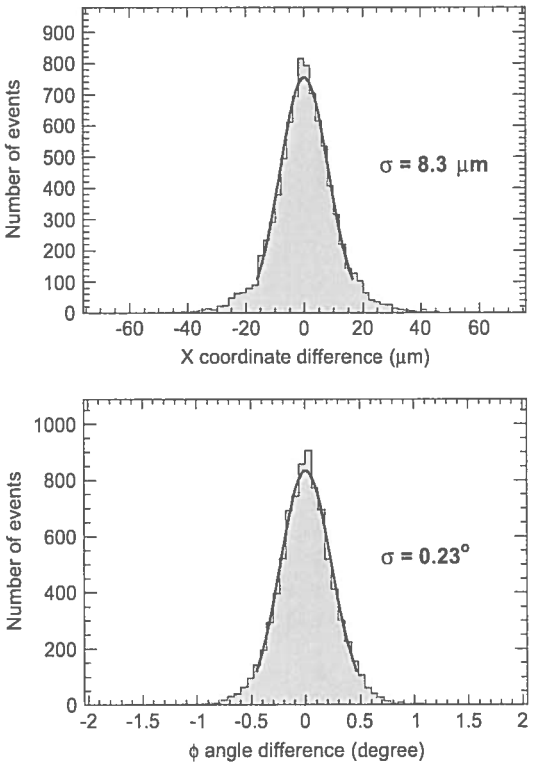

Fig. 7. Distributions of difference between reconstructed "*odd*" and "even" tracks *X* coordinates (top) and ϕ angles (bottom) divided by factor of 2. Histograms are test beam data with the prototype filled with DME-based mixture, beam incident angle 30°. Solid lines represent Gaussian fits applied to the central parts of distributions.

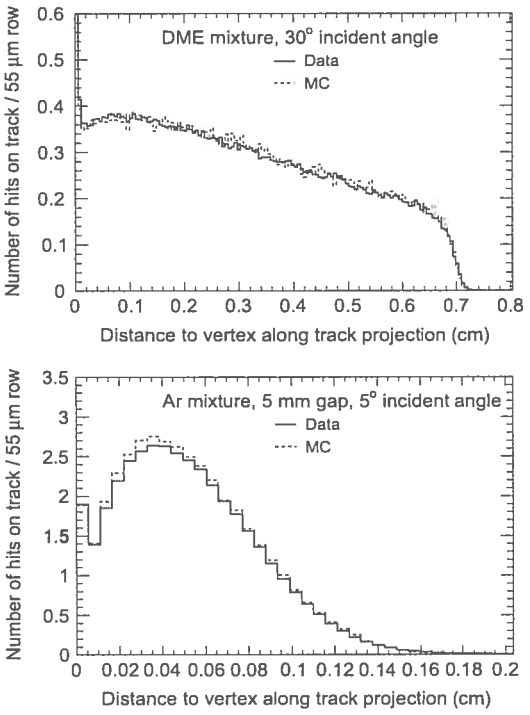

Fig. 8. Comparison of data and MC longitudinal track profiles. Top: DME-based mixture, 30° angle with incident beam. Bottom: Ar-based mixture, 5 mm gap, 5° incident angle.

ATLSIM [21] packages for description of the test beam set-up, detectors geometry and ionization losses in gas. Particle ionization losses are simulated with high precision using the Photo-Absorption Ionization (PAI) model [22]. The simulations include all main detection specific features like electron drift processes in gas, electron amplification and front-end electronics response.

There were two parameters in MC which needed to be tuned. One of them was an effective threshold of pixel discriminator. It was tuned to fit the total number of fired pixels on a particle track and was found to be 0.9 of primary ionization electrons for DME-based mixture and 0.56 electrons for Ar-based mixture. The effective threshold is defined as the number of primary electrons needed to develop signal above the front-end electronics threshold. As it was mentioned in Section 2 the pixel discriminator threshold was set to 600 electrons and the chambers were operating at the gas gain of 1500–2000. If full charge is collected then this would correspond to the effective threshold of 0.3–0.4 primary electrons. However, the largest part of the collected charge is defined by the drift of positive ions in the amplification gap and only fraction of the total charge is translated to the signal amplitude after its shaping (amplifier integration time is about 100 ns). The smaller ion drift velocity (the larger ion mass) the less charge is used for signal. That is why for the DME gas the effective threshold is larger than for the Ar-based mixture.

The other parameter tuned was the electron attachment coefficient in the DME-based gas mixture (oxygen contamination in premixed gas). This effect leads to a dependence of a number of ionization electrons which reach amplification region on the drift distance decreasing the number of fired pixels with larger *Z* coordinate. The best agreement was achieved for a mean absorption path of drifting electrons of 9.5 mm. Using these corrections and parameters presented in Table 1, excellent agreement between data and MC was achieved in the number of fired pixels and their distributions along and transverse to the track projection on the chip plane.

Fig. 8 shows examples of longitudinal track profiles – the number of fired pixels along the track projection – for different gas mixtures and incident angles of beam particles.

Fig. 9 compares data and MC distributions of the perpendicular distance of fired pixels from the track projection on the chip plane. The shape and the absolute scale of longitudinal and transverse profiles depend on many different factors: number of primary ionization electrons, drift and amplification processes, pixel signal shaping, threshold, etc. The agreement between data and simulation manifests the quality of the GasPixel Monte Carlo model and good understanding of the processes in the detector.

Fig. 10 compares data and MC distributions of the mean number of fired pixels on reconstructed tracks for all three GasPixel prototypes and different incident angles.

5. Results and discussion

The accuracy of the reconstructed track vertex in the direction perpendicular to the track projection (*X*-coordinate accuracy) as a function of the particle incident angle for DME-based and Ar-based mixtures is shown in Figs. 11–13. Both data and MC simulation results are presented. One sees that the coordinate accuracy strongly depends on the incident angle and diffusion properties of the gas mixture. With increase of incident angle both track projection length and number of fired pixels grows up leading to better accuracy. For DME-based mixture the coordinate accuracy varies from 10 μm to 8 μm when the incident angle changes from 5° to 30°. Because of significantly larger electron diffusion this dependence is much stronger for Ar-based mixture. For the same chamber geometry (10 mm drift gap) the coordinate accuracy varies from 45 μm to 27 μm depending on the incident angle. Comparing Figs. 12 and 13 one can also

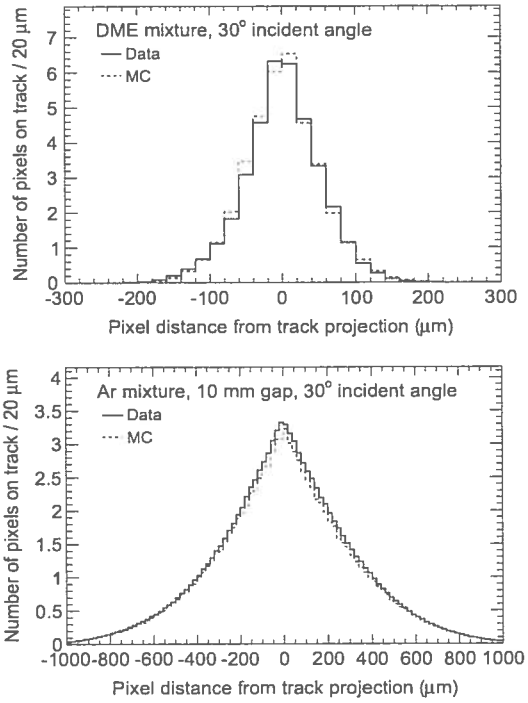

Fig. 9. Comparison of data and MC transverse track profiles. Top: DME-based mixture, 30° angle with incident beam. Bottom: Ar-based mixture, 10 mm gap, 30° incident angle.

conclude that the coordinate accuracy is approximately the same for the same track projection length (10° and 20° incident angles for 10 and 5 mm gaps correspondingly).

These results also show that despite large diffusion coefficients and low ionization density in the Ar-based mixture one still obtains very good coordinate accuracy of 30–40 μm. The record coordinate accuracy for gaseous detectors of 8 μm was achieved with low diffusion DME-based gas mixture.

Figs. 14–16 give the results of measurements of the angular resolution of the track projection on the chip plane. As expected, accuracy depends very strongly on the track projection length (or on the particle incident angle) and diffusion properties of the gas. For low diffusion DME-based mixture angular accuracy of about 0.2° (or 3.5 mrad) was achieved for 30° particle incident angle. This value corresponds to ~17% momentum resolution for the particle with transverse momentum p_T=20 GeV if such a detector is placed in a magnetic field of 2 T at the distance of 1 m from primary vertex. Calculations show that this momentum resolution is practically independent of incident particle angle.

For complete reconstruction of the track segment the angle in the plane perpendicular to the pixel chip has to be measured. Figs. 17–19 present the reconstruction accuracy of the angle θ between the particle trajectory and the chip plane. For the DME-based mixture the angular accuracy varies from 0.3° to 1.1° for incident angle variation from 30° to 5° correspondingly. For Ar-based mixture in the chamber with the same geometry (10 mm drift gap) the variation of angular accuracy is from 1.3° to 1.5° and it is larger (from 3.5 to 4.7°) for 5 mm drift gap. The reason why the θ angle accuracy becomes worse with increase of incident angle is pure geometrical: projection of measurement error in drift direction on θ angle is larger for inclined (bigger θ) track.

The accuracy of θ angle measurement is defined not only by diffusion but also by electron drift velocity and electronics parameters. The Timepix-1 chip electronics has a rather slow rise time (~100 ns) and at large signal amplitude fluctuations it has

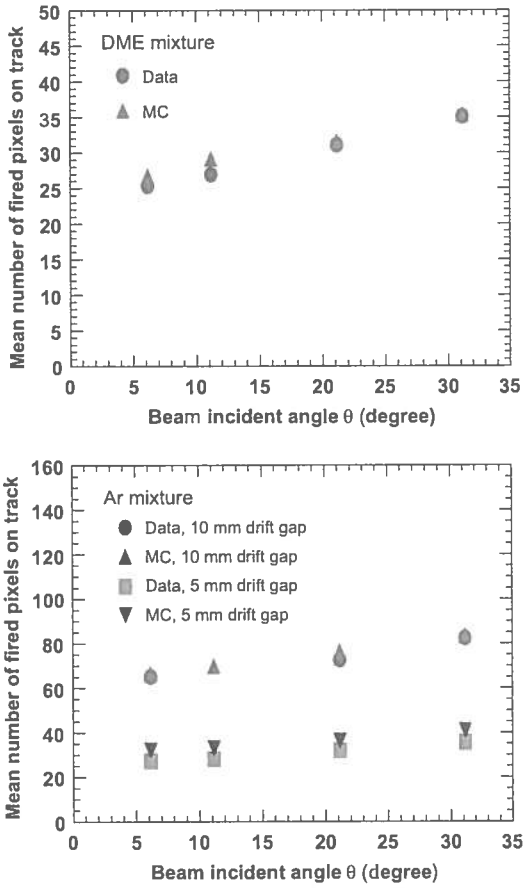

Fig. 10. Data and MC comparison for mean number of pixels on track. Results for different prototypes and angles with beam axis are presented: top – for 10 mm gap prototype with DME-based mixture, bottom – for 5 and 10 mm gap prototypes with Ar-based mixture.

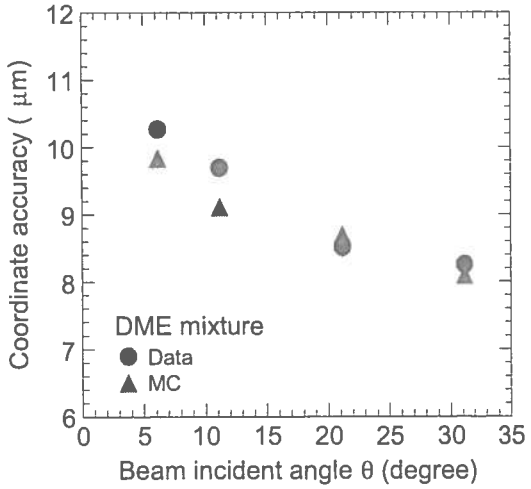

Fig. 11. Data and MC comparison of X coordinate reconstruction accuracy for different beam angles for the detector prototype with DME-based gas mixture.

significant impact on the drift time measurement accuracy. Contribution of this effect to the angular accuracy is higher for the gases with high electron drift velocity. Discrepancy between data and MC in the accuracy of θ angle reconstruction most likely is due to not exact electronics signal representation in the MC simulation. The signal from the chamber consist of a fast electron component

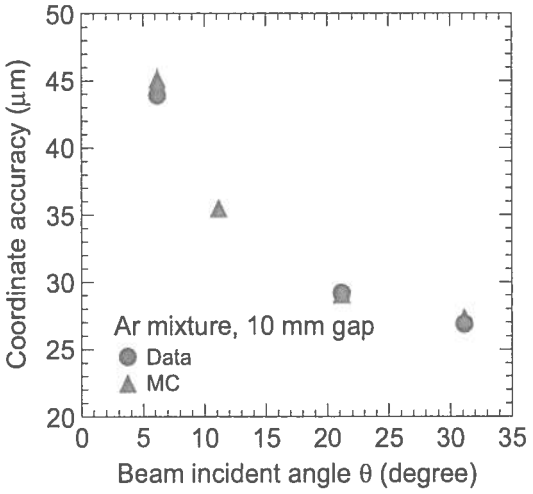

Fig. 12. Data and MC comparison of X coordinate reconstruction accuracy for different beam angles for the detector prototype with 10 mm drift gap and Ar-based gas mixture.

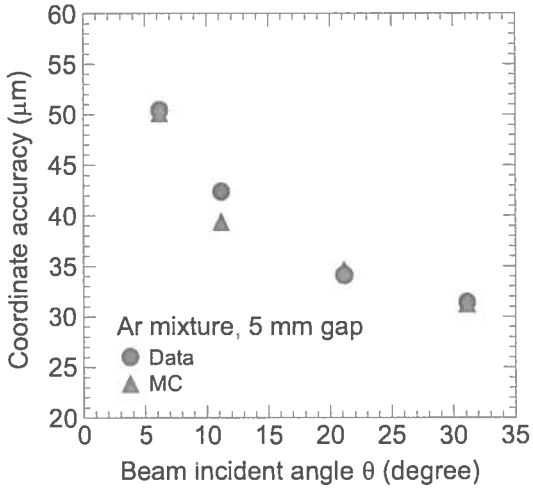

Fig. 13. Data and MC comparison of X coordinate reconstruction accuracy for different beam angles for the detector prototype with 5 mm drift gap and Ar-based gas mixture.

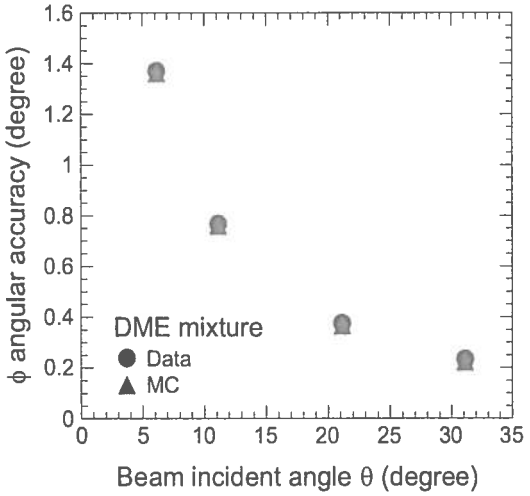

Fig. 14. Data and MC comparison for reconstruction accuracy of ϕ track angle in chip plane for different beam angles for the detector prototype with DME-based gas mixture.

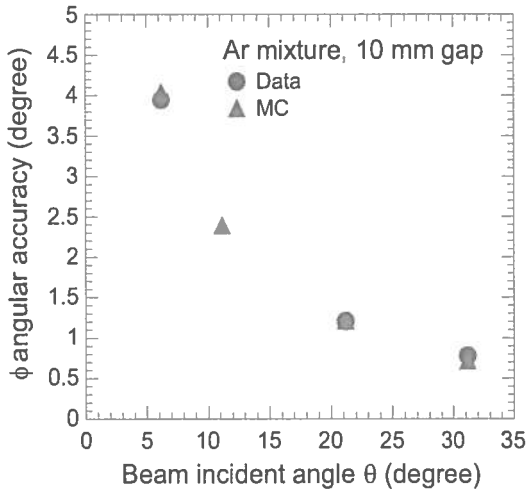

Fig. 15. Data and MC comparison for reconstruction accuracy of ϕ track angle in chip plane for different beam angles for the detector prototype with 10 mm drift gap and Ar-based gas mixture.

and a slow ion component. Exact parameters of this signal depend on gas composition, voltage and chamber geometry and are not known precisely enough. Misrepresentation of the exact signal shape in the MC leads to a different contribution of the time-walk effect to the drift time measurement accuracy in the data and MC and, hence, to different errors in the coordinate measurement in the vertical plane. This effect does not affect the measurements in the pixel chip plane.

For development of a realistic GasPixel detector it is important to understand how pixels size affects the measurement accuracy. It is clear that in case of low diffusion gas mixture when the spatial accuracy is at the level of 10 μm an increase of the pixel size will affect this resolution. For the gases with rather large diffusion like Ar-based mixtures the effect might not be that essential and one can significantly reduce a number of channels increasing pixel size without affecting the detector performance. Fig. 20 shows the Monte Carlo simulation of the effect of the pixel size on tracking performance of the GasPixel detector filled with Ar-based mixture. One sees that the increase of the pixel size from 50×50 to 100×100 μm^2 changes the X coordinate accuracy by 5 μm and for 100×200 μm^2 one obtains resolution of 47 μm. It is interesting to note that the increase of the pixel size up to 300×300 μm^2 practically does not affect angle measurement accuracy. This reflects the fact that angle measurement accuracy is largely defined by transverse diffusion which for Ar-based mixture is 430 μm for 1 cm drift length (see Table 1).

6. Conclusions

Tracking properties of the GasPixel detectors with different geometries and different gas mixtures were studied. The results demonstrate very high potential of this type of detectors for precise track measurements. For low diffusion DME-based gas mixture a coordinate accuracy of 8 μm and angular accuracy of 0.2° in chip plane were achieved. These values are the best results obtained for gaseous tracking detectors. Being placed in the inner tracking volume of the collider experiment with a magnetic field of 2 T at a radius of 1 m from the interaction point, such a detector would allow the reconstruction of the momentum of the particle with p_T=20 GeV with accuracy of about 17% using only one

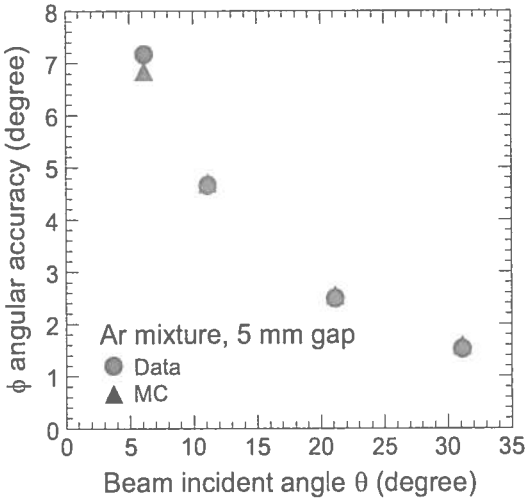

Fig. 16. Data and MC comparison for reconstruction accuracy of ϕ track angle in chip plane for different beam angles for the detector prototype with 5 mm drift gap and Ar-based gas mixture.

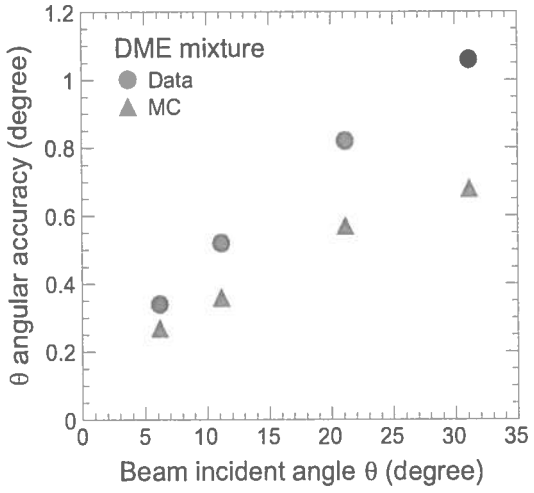

Fig. 17. Data and MC comparison for reconstruction accuracy of θ track angle in plane orthogonal to the chip for the detector prototype with DME-based gas mixture.

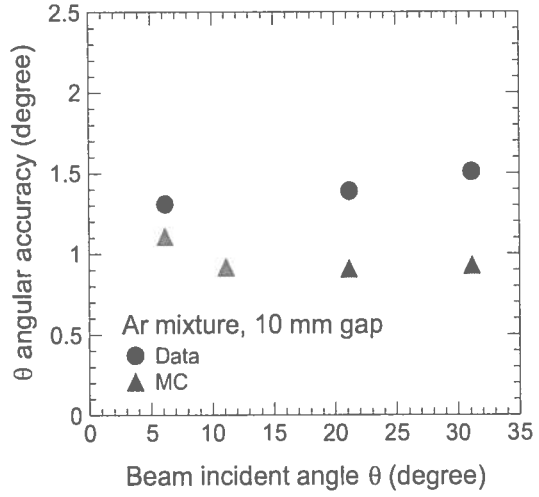

Fig. 18. Data and MC comparison for reconstruction accuracy of θ track angle in plane orthogonal to the chip for the detector prototype with 10 mm drift gap and Ar-based gas mixture.

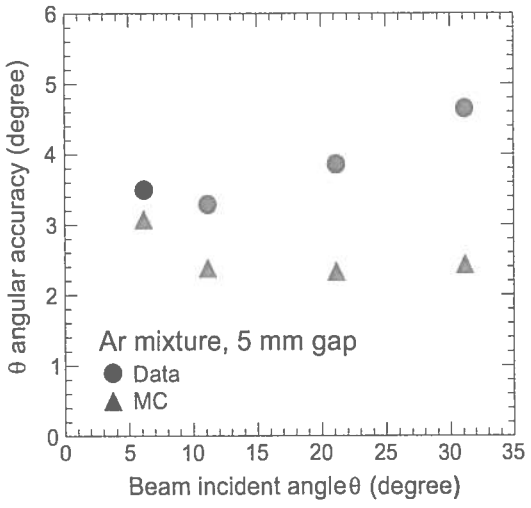

Fig. 19. Data and MC comparison for reconstruction accuracy of θ track angle in plane orthogonal to the chip for the detector prototype with 5 mm drift gap and Ar-based gas mixture.

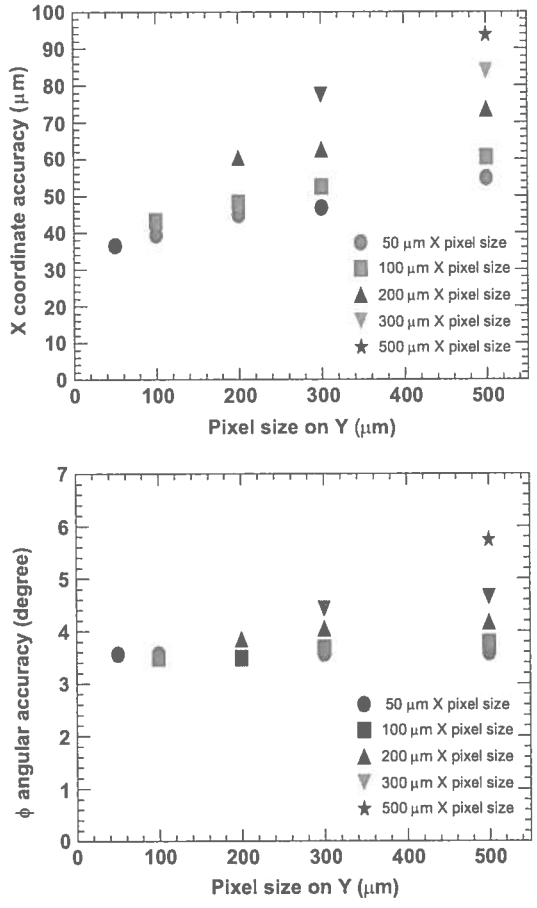

Fig. 20. Monte Carlo simulation of a GasPixel detector with 5 mm drift gap and Ar based mixture, 20° incident angle. Spatial (top) and angular (bottom) accuracy for different pixel sizes are shown.

detector plane. Angular accuracy in the plane perpendicular to the chip of 0.3–1.0° was obtained. This parameter can be significantly improved using faster electronics. For Ar-based mixture the spatial accuracy is 27–50 μm, depending on the incident angle. Angular resolution in the chip plane is 0.8–7.2°. It strongly depends on

track projection length. For Ar-based mixture the increase of the pixel size from 50×50 to $100 \times 200\ \mu m^2$ with corresponding reduction of electronics channel number would not significantly compromise the tracking performance of the GasPixel detectors.

Acknowledgments

We thank CERN SPS staff for the successful operation of the accelerator during the test beam period. This work was partially supported by Russian Ministry of Education and Science –Contract no. 11.519.6029, and also by Russian Foundation for Basic Research – Grant no. 14-22-03053. We also thank Christoph Rembser for his support of the work.

References

[1] H.-G. Moser, Progress in Particle and Nuclear Physics 63 (2009) 186.
[2] A. Nomerotski, Nuclear Instruments and Methods in Physics Research Section A 598 (2009) 33.
[3] ATLAS Collaboration, ATLAS Letter of Intent Phase-II Upgrade, CERN-2012-022, LHCC-I-023, 2012.
[4] R. Bellazzini, et al., Nuclear Instruments and Methods in Physics Research Section A 535 (2004) 477.
[5] M. Chefdeville, et al., Nuclear Instruments and Methods in Physics Research Section A 556 (2006) 490.
[6] V. Blanco Carballo, et al., Journal of Instrumentation 5 (2010) 02002.
[7] V. Blanco Carballo, et al., Nuclear Instruments and Methods in Physics Research Section A 629 (2011) 118.
[8] F. Hartjes, et al., Nuclear Instruments and Methods in Physics Research Section A 706 (2013) 59.
[9] W.J.C. Koppert, et al., Nuclear Instruments and Methods in Physics Research Section A 732 (2013) 245.
[10] K.A. Olive, Particle Data Group, Chinese Physics C 38 (2014) 090001, chapter "Micro-Pattern Gas Detectors".
[11] K.A. Olive, Particle Data Group, Chinese Physics C 38 (2014) 090001, chapter "Time-projection chambers".
[12] Y. Giomataris, et al., Nuclear Instruments and Methods in Physics Research Section A 376 (1995) 29.
[13] R. Schön, et al., Nuclear Instruments and Methods in Physics Research Section A 718 (2013) 446.
[14] J. Kaminski, et al., Journal of Physics: Conference Series 460 (2013) 012004.
[15] R. Bellazzini, et al., Nuclear Instruments and Methods in Physics Research Section A 579 (2007) 853.
[16] X. Llopart, et al., Nuclear Instruments and Methods in Physics Research Section A 581 (2007) 485.
[17] A. Kruth, et al., Journal of Instrumentation 5 (2010) C12005.
[18] S. Biagi, R. Veenhof (http://magboltz.web.cern.ch/magboltz/); R. Veenhof (http://garfield.web.cern.ch/garfield/).
[19] T. Akesson, et al., Nuclear Instruments and Methods in Physics Research Section A 485 (2002) 298.
[20] R. Brun, et al., CERN Publication DD/EE/84-1, 1992; CN Division Application Software Group, CERN Program Library Long Writeup W5013, 1993.
[21] A. Artamonov, et al., DICE-95, ATLAS Internal Note, ATLAS-SOFT/95-14, CERN, 1995.
[22] V.M. Grishin, V.K. Ermilova, S.K. Kotelnikov, Nuclear Instruments and Methods in Physics Research Section A 307 (1991) 273.